



# Revolutionizing Waste Management: Solidification of Landfill Leachates Using Alkali-Activated Slag

Thandiwe Sithole<sup>1</sup> · Lisakhanya Jobodwana<sup>1</sup> · Felicia Magedi<sup>1</sup>

Accepted: 12 August 2024  
© The Author(s) 2024

## Abstract

Landfill leachate is a highly hazardous effluent characterized by a high concentration of recalcitrant pollutants, presenting a significant environmental challenge. This study investigated the solidification of landfill leachate contaminants using sodium hydroxide-activated Granulated Blast Furnace Slag (GBFS). The stability of the resulting geopolymer was evaluated through unconfined compressive strength and leaching tests. Optimal curing conditions were identified as 7 days at a sodium hydroxide concentration of 12 M, achieving an unconfined compressive strength of 45.738 MPa at a liquid-to-solid ratio of 15%. A linear relationship was observed between the liquid-to-solid ratio and flow workability, with maximum flow workability evidenced by an average diameter of 242 mm at a liquid-to-solid ratio of 0.25. However, a minimum liquid-to-solid ratio of 0.15 was necessary to obtain a workable mortar. The produced geopolymers were characterized using X-ray Fluorescence (XRF) for mineralogical analysis, Scanning Electron Microscopy (SEM) for morphological examination, and the Toxicity Characteristic Leaching Procedure (TCLP) for leaching tests. The findings demonstrated the successful solidification of landfill leachate using GBFS geopolymer. The leachability tests revealed that the geopolymer did not release metals in concentrations exceeding the allowable limits set by the United States Environmental Protection Agency (USEPA), indicating effective encapsulation of the pollutants within the geopolymer matrix. Furthermore, the resultant geopolymer brick is eco-sustainable and can be classified as a green construction material.

**Keywords** Geopolymerization · Granulated Blast Furnace slag · Landfill Leachate Concentrate Contaminant · Solidification/stabilization · Unconfined Compressive Strength

## 1 Introduction

Solid waste disposal is a challenge faced internationally, mostly in underdeveloped nations. As industrialization advances, handling waste in urban regions affects residents' health and the environment [27]. The various waste management options vary with management approaches, from waste retreat and reduction to reuse, recycling, recovery, and treatment and disposal. In South Africa, the frequent technique of waste disposal is landfilling, with about 90% of waste disposed of at landfills [26]. A landfill is a waste disposal facility that has been constructed with specialized pollution

control technology to lessen possible hazards. Landfills are typically found above the ground [32]. This way of trash disposal is found to be easy and low-cost in many places [1]. In the process of landfilling, a landfill leachate is produced. Landfill leachate concentrate is a very hazardous effluent with a high concentration of recalcitrant pollutants. Despite the advantages of a landfill, the existence of hazardous inorganic and organic elements in the leachate [11] and badly constructed solid waste management facilities represent a substantial threat to numerous sectors of the environment. When landfill leachate is not gathered, cleaned, and disposed of correctly, it will pollute the soil, surface water, and groundwater [5]. As a result, landfill leachate is acknowledged as a significant environmental issue.

Many developing nations manage landfills lacking sufficient leachate collection and treatment systems, which has negative environmental consequences. The type of leachate affects how strong the effect is [1]. Leachate compositions are different regarding trash type, moisture, oxygen

✉ Thandiwe Sithole  
nastassias@uj.ac.za

<sup>1</sup> Department of Chemical Engineering, University of Johannesburg, P.O. Box 17011, Doornfontein 2028, South Africa

availability, and age [10]. Soil pollution by leachate has a considerable effect on soil standards. According to [23], the soil is the most contaminated portion of the environment surrounding landfills since chemical compounds are transferred and disseminated when water percolates through it. Heavy metals, polyaromatic hydrocarbons, and pharmaceutical chemicals are among the contaminants that build up in soil [37]. The implications of these contaminants, particularly heavy metal contamination, are a source of worry when it comes to agriculture [23].

Although several landfill leachate concentration treatment systems have been explored, most of them are challenging to execute. With a large salt concentration, reinfiltrating the leachate into the landfill body is unsustainable [36]. The more radical treatment methods, such as membrane treatment, thermal incineration, or drying, cannot entirely remove all pollutants. Due to cost constraints, advanced oxidation and other non-harmful treatment technologies are severely limited [43].

Solidification/stabilization is a scientific and economical clean-up technology in which the pollutants of landfill leachate concentrate can be encapsulated in one stage to ensure zero wastewater emission, allowing the binder to be reused and safely disposed of. The commonly utilized binder in solidification/stabilisation procedures is Portland cement. Numerous studies have demonstrated that Portland cement effectively stabilizes various pollutants, including heavy metals like zinc, lead, cadmium, and chromium, ensuring they meet the minimum safety requirements in their solidified form [15, 22]. Unfortunately, Portland cement manufacturing demands a great amount of energy and is accountable for 5–10% of anthropogenic  $CO_2$  emissions, prompting a variety of attempts to minimize its use [17]. Furthermore, the high pore water pH of PC (often  $> 13$ ) increases the kinetic energy of several heavy metals [7]. Portland cement is recognized to be inefficient when pollutants are not restricted to inorganics and should be utilized with extreme vigilance [29]. Portland cement also exhibits poor durability and curing ability due to the presence of ammonium nitrogen and chloride ions, and it is prone to dissolution [43].

The substitution of Portland cement with industrial byproducts is important to decrease environmental effects and enhance material qualities such as reduced permeability, a greater buffering capacity, and reduce leachability. There is a need to develop a low-cost neutralizing agent that can counteract armoring and low-carbon binders to eliminate numerous harmful wastes [9].

In recent years, the solidification of high-concentration waste, including landfill leachate, through geopolymerization has gotten significant attention. Research indicates that geopolymers offer excellent performance characteristics compared to Portland cement. The zeolite-like structure of

geopolymers can effectively immobilize organics, such as ammonium nitrogen, present in the waste [42]. For instance, a study demonstrated that using blast furnace slag-based geopolymer for solidifying landfill leachate achieved a high solidification efficiency, with stabilization rates of heavy metals reaching approximately 99% [43]. Another study by Zhang et al. [44] explored the use of fly ash-based geopolymers for the same purpose, revealing that the developed geopolymer exhibited excellent stability, high contaminant removal, and solidification rates of organic matter and ammonium nitrogen up to 93% and 91%, respectively. The resulting geopolymer also displayed good compressive strength, suggesting its potential as a novel building material. Despite the promising results of geopolymerization for the solidification of landfill leachate, research in this area remains limited. Therefore, our study aims to investigate the solidification of landfill leachate using granulated blast furnace slag geopolymers.

According to the National Waste Information Baseline report, around 5.4 million tonnes of slag are generated yearly in South Africa, with approximately 50% getting recycled and the remaining being thrown off in heaps and landfills [4]. This causes an environmental problem and takes up a lot of space when landfilled. This problem associated with Granulated blast furnace slag (GBFS) calls for an innovative solution to be beneficial, solve problems associated with waste disposal and develop a value-added product. This research investigates the possibility of using waste material, specifically GBFS, to create a geopolymer that can be used as a neutralizing medium to remediate landfill leachate in a single process. In addition, the mentioned waste material will be used to create building materials. Geopolymers have been used successfully in remediating landfill leachate contaminants, but the literature is limited. The aim of this study was to solidify landfill leachate concentrate using alkali-activated GBFS geopolymers and investigate the possibility of using the produced geopolymers as construction materials.

## 2 Method and Material

### 2.1 Materials

Granulated Blast Furnace Slag (GBFS) was collected from ArcelorMittal South Africa. Sodium hydroxide (NaOH) was used as an alkaline activator. NaOH was supplied by Glass World. Landfill leachate was supplied by the Robinson Deep landfill site in Johannesburg.

## 2.2 Equipment

The chemical composition of the GBFS, landfill leachate, and geopolymers that were produced was determined by XRF (Rigaku ZSX Primus II). The mineral phases of the raw materials and the geopolymer-landfill leachate concentrate were identified by XRD (Ultima IV Rigaku). The FTIR (Thermo scientific Nicket IS10) was utilized to determine the absorption bands of the raw materials and the resulting geopolymer landfill leachate. Scanning electron microscopy (SEM Tescan Vega 3X MU1) images were taken to study the surface morphology of raw materials and the produced geopolymers. The unconfined compressive strength (UCS) of raw materials and the produced geopolymer species were determined using a cyber plus compression machine. A test table was used to determine the workability of the paste.

## 2.3 Synthesis of the Geopolymer

The alkali activator solution was produced by dissolving 6 wt% sodium hydroxide and 16 wt% powdery sodium hydroxides in landfill leachate concentrate. The use of a high-purity (98%), analytical-grade NaOH was used to prepare the alkali activation solution. The alkali activator solution was stored for 12 h to improve sodium hydroxide polymerisation. The alkali activator solution was then blended with 300 g of GBFS to produce a homogeneous paste. The paste was then transferred into a steel mould (50×50×50 mm) and placed on an oscillating table to clear bubbles. Finally, the mould was wrapped in plastic wrap and placed in an 80° C oven for 24 h to cure [19]. The cured body was sealed and cured at room temperature after demoulding after 28 days of curing and used for subsequent determinations. Different concentrations of alkaline activators (3 M, 6 M, 9 M, and 12 M) were used for comparison. The experiments were done in triplicates, and the average was taken. This was shown by the error bars on the figures.

## 2.4 Effect of Alkali Content on UCS

The alkaline activator Sodium hydroxide was mixed with landfill leachate concentrate to form a solution. Different concentrations (3 M, 6 M, 9 M, and 12 M) of Sodium hydroxide powder solution were prepared. The solutions were left at room temperature for 24 h to cool down before using them.

## 2.5 Effect of Liquid/Solid Ratio on UCS

Each sample from sample S1 to S4 was mixed with different amounts of Sodium hydroxide solution. Amounts of 10%, 15%, 20% and 25% were used.

## 2.6 Effect of Curing Time on UCS

The composites were subjected to different curing days for 1, 3 and 7 days. The UCS was used to determine the optimum curing day.

## 2.7 Flow Workability

The flow workability was determined using a flow table test with a cone with a bottom diameter of 100 mm, a height diameter of 60 mm, and a top diameter of 70 mm. The cone and flow table were first wiped down with a wet cloth. The cone was then placed in the middle of the flow table instrument and filled with the alkali-activated paste into two layers. Each layer was tempered 20 times with a tamper to compact the paste uniformly. In the second layer, the paste was levelled up and lifted vertically. The flow table was dropped 25 times. The flow workability was determined by measuring the diameter of the paste on the flow table along the four lines. The diameters were measured in millimetres, and the average was computed.

## 2.8 Leaching Test

The toxicity characteristic leaching technique was used for the leaching test. The hardened corpses were first broken into small pieces and filtered through a 0.95 cm sieve. The extraction fluid was then transferred to a 1 L extraction bottle with 50 g of solids at a solid-to-liquid ratio of 20:1 (L/kg). 5.9 mL acetic acid was dissolved in 1.0 L de-ionised water to make the extraction fluid. At 25 degrees Celsius, the mixture was spun at 30 rpm for 18 h. Individual samples were vacuumed and filtered with a 0.45 m pickling glass fibre filter before being stored at 4 degrees Celsius.

## 2.9 UCS Testing

The UCS of the geopolymer specimen was determined by loading the specimens into a cyber plus compression machine with a maximum load capacity of 100 kN and applying a constant displacement rate of 2 mm/min until the geopolymer specimen failed.

## 2.10 Toxicity Characteristic Leaching Procedure (TCLP)

The environmental impact of the produced geopolymer brick was investigated using TCLP. TCLP was conducted following the United States Environmental Protection Agency method (USEPA). The leachability of GBFS was determined using an extraction buffer of acetic acid and sodium hydroxide (pH 4.93 ± 0.05) at a liquid/solid ratio of

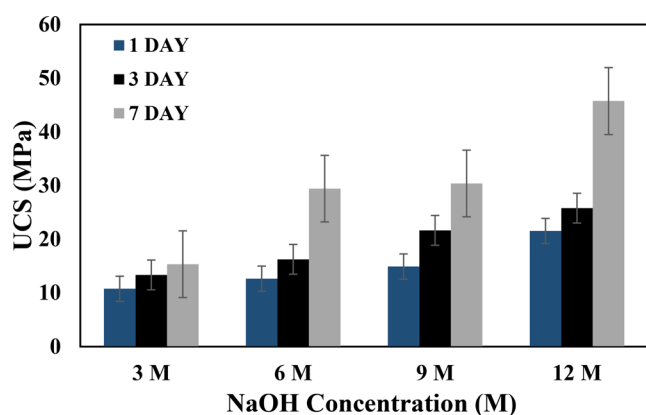


**Fig. 1** Effect of activator concentration and curing time on UCS of the geopolymer

20:1 [45]. A thermostatic shaker was used for the extraction and was subjected to 24 h shaking at  $25 \pm 2$  C. After 24 h, two samples were taken per test conducted and filtered. The leachate was analyzed using ICP to determine the concentration of leached metals.

### 3 Results and Discussion

#### 3.1 Effect of Alkali Content and Time on UCS

Figure 1 depicts the influence of varying NaOH concentrations on UCS. As illustrated in the graph, increasing NaOH concentration from 3 to 12 M increases the UCS of the alkali-activated GBFS-based sample. Increasing the concentration from 3 to 6 M resulted in a 63.50% increase in UCS; from 9 M to 12 M, there was a 67.44% increase in UCS. The rising trend is primarily the result of the high leaching rate of silica and alumina (Part, Ramli and Cheah, [28]). It is worth noting that a concentration exceeding 15 M is hostile-friendly. Any concentration of alkaline activator above 13–15 M is no longer user-friendly; hence, the concentration was varied until 12 M. Furthermore, increasing the molar concentration of alkaline solution reduces workability and compressive strength and increases the likelihood of efflorescence [16, 31]. Identical patterns have been revealed by (Sithole, Okonta and Ntuli, [33] Sithole and Mashifana [16, 34].

The effect of curing time (1, 3 and 7 days) at different NaOH concentrations is also depicted in Fig. 1. It has been discovered that the curing period is crucial in forming UCS. Direct proportionality was observed between UCS and curing age as UCS increases as the curing days increase. This trend corroborates the findings by Das et al. [8]. The increase in UCS with curing time is due to the curing period's extent of aluminosilicate species dissolution and an acceleration of the development of a hardened sample, especially during

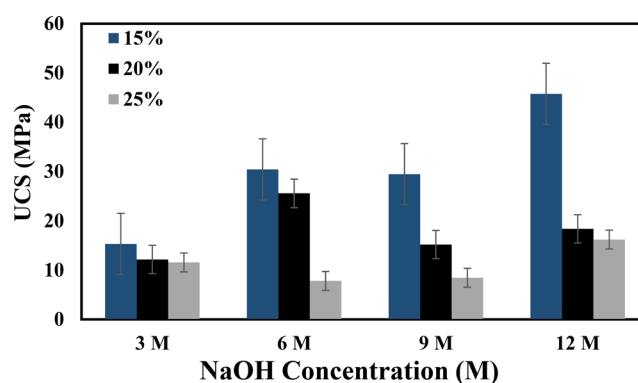


**Fig. 2** Effect of Liquid/ Solid ratio (L/S) on UCS (cured for 7 days)

the beginning stages of the alkaline activation process. With increasing curing time, Si, Al, and Na components were balanced, allowing undissolved GBFS particles to react with the alkaline solution [24]. Elongated curing produced more steady reaction products, resulting in a denser microstructure with enhanced mechanical effectiveness and UCS [3, 24]. Furthermore, the  $\text{SiO}_2/\text{Al}_2\text{O}_3$  molar ratio may be inside the allowed range, resulting in higher levels of soluble silica (Si-O-) and  $\text{Na}_2\text{O}$ .

#### 3.2 Effect of Liquid/Solid Ratio on UCS and Flow Workability

##### 3.2.1 Effect of Liquid/Solid Ratio on UCS

Figure 2 demonstrates the impact of changing the L/S ratio on the UCS from 15 to 25%. A low L/S ratio of 10% produced a paste that was too dry to cast due to its low workability. Alkali-activated pastes prepared with a 15% L/S ratio had the best workability, with the highest UCS of 45.738 MPa. This is hypothesized to be attributable to the uniformity of the paste at 15%, which enables the dissolution of Silicon and Aluminium from GBFS whilst also preventing polycondensation during the GBFS alkaline activation process [21]. A decrease in UCS was observed when the L/S was increased to 25%. This is due to the low gel formation and separation within the paste, which made it hard to mould, as well as its low workability, meaning it was too wet, which made it challenging to mould [40]. Furthermore, exceeding the ideal L/S ratio decreases the porous structure in the hardened paste, which decrease the mechanical properties of the alkali-activated GBFS samples [40]. These observations and findings corroborated with previous research conducted by [34, 35]; Falayi et al., [12] Jafari Nadoushan and Ramezani-pour, [16] Falayi, Okonta, and Ntuli, [13]. Increasing the liquid-to-solid ratio yields an impoverished alkaline ambience, and the extent of alkaline activation and

gelation lowers, resulting in mechanical performance degradation [40].

### 3.2.2 Effect of Liquid/Solid Ratio on Flow Workability

Figure 3 depicts the flow workability results for various L/S ratios. It is clear that the larger the L/S ratio, the larger the mortar spread value (diameter). According to other authors, the correlation between L/S and workability is linear (Chindaprasirt, Buapa and Cao, [6]). This study needed a minimum L/S of 0.15 to acquire a GBFS mortar. The L/S ratio of 0.1 indicated that there was no flow of the paste and that it was not viscous, as evidenced by the graph, and it has the lowest flow workability with an average diameter of 85.33 mm. These findings are consistent with Fig. 2's findings on the effect of L/S on UCS, as the 0.1 ratio was not tested for compressive strength because the paste was too dry and had low flow workability to be moulded. Particularly, the higher the binder (GBFS) material of the mortar (or lower the aggregate content), the higher the NaOH concentration required to produce a good paste. This is because while the aggregate absorbs some NaOH concentration, the binder absorbs most of it. As in GBFS mortars, the greater the liquid-to-solid ratio, the greater the spread at each specimen. This is attributed to the excess liquid, which reduces the mixture's viscosity, making it easier to spread. However, the excess liquid also forms voids within the geopolymer matrix, consequently leading to a decrease in UCS [14], as illustrated in Fig. 2.

### 3.3 X-Ray Fluorescence (XRF)

Table 1 shows the XRF results, which indicate that four samples share the same metal oxide content, except for the raw material GBFS, which has NiO in Table 1. CaO, SiO<sub>2</sub>, and Al<sub>2</sub>O<sub>3</sub> account for most of GBFS with weight% of 44.40%, 30.08% and 10.82%, respectively, matching the findings of (Yildirim et al., [46]). It is worth noting that Calcium oxide (CaO) in GBFS in this study is greater than other compounds, which was observed in the literature (Wardhono, Law and Strano, [39]; Yildirim et al., [46]). Because Ca<sup>2+</sup> encourages the creation of crystal structures at high temperatures, the existence of Ca<sup>2+</sup> in the geopolymer may greatly affect the formation of geopolymer gels (Ye, Zhang and Shi, [41]). CaO from slag acts as a setting agent, hardening the product at 25°C without impacting its mechanical characteristics. It is apparent that the amount of Na<sub>2</sub>O increases as concentration increases, whereas the amount of SiO<sub>2</sub> decreases as concentration increases. The increase in alkali content promotes the dissolution of silicon and aluminium in the solution, thereby enhancing the compressive strength of the sample. This effect is particularly noticeable

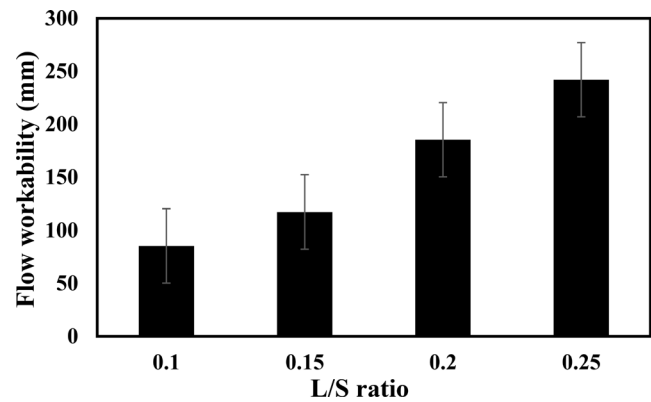


Fig. 3 Effect of Liquid/Solid ratio on Workability

Table 1 Chemical composition of the geopolymers at different activator concentrations

Chemical Compositions	GBFS	3 M	6 M	9 M	12 M
Na <sub>2</sub> O	0.1742	1.3140	1.6157	3.1551	7.7883
MgO	4.0611	2.0491	1.9625	1.5641	1.7807
Al <sub>2</sub> O <sub>3</sub>	10.8286	8.4226	8.5480	7.4981	7.0772
SiO <sub>2</sub>	30.0800	25.0781	24.5051	22.4110	22.1935
P <sub>2</sub> O <sub>5</sub>	0.0119	0.0362	0.0319	0.0215	0.0217
SO <sub>3</sub>	2.1717	1.9169	1.8170	1.8509	1.1724
Cl	0.0708	1.2852	0.1697	0.1434	0.1724
K <sub>2</sub> O	1.1426	1.9104	1.3484	1.3024	1.2320
CaO	44.4015	50.2966	50.0723	51.3440	48.1093
TiO <sub>2</sub>	1.0458	0.0793	1.5883	1.5601	1.4308
Cr <sub>2</sub> O <sub>3</sub>	0.0418	4.7157	0.0935	0.0728	0.2512
MnO	4.0984	2.0415	5.5924	6.1321	5.4301
Fe <sub>2</sub> O <sub>3</sub>	1.1542	0.3664	1.8238	1.9523	1.8422
SrO	0.2574	0.0270	0.3807	0.4200	0.3868
Y <sub>2</sub> O <sub>3</sub>	0.0185	0.0947	0.0279	0.0285	0.0283
ZrO <sub>2</sub>	0.0840	0.3664	0.0854	0.1005	0.1089
BaO	0.3297	0.0000	0.3375	0.4430	0.3638

as the concentration of NaOH increases; the concentrations of silicon and aluminium correspondingly decrease. This shows that the alkaline activation process was occurring and that SiO<sub>2</sub> was reacting (Sithole and Mashifana, [33]). The Na<sub>2</sub>O content increased because of the increasing concentrations of sodium hydroxide used (activator). At a NaOH concentration of 3 M, the BaO content is observed to be zero. This may be because, at low concentrations of NaOH, BaO completely reacts with the contaminants found in the landfill leachate, immobilizing them within the geopolymer matrix [25]. Moreover, the amount of SO<sub>3</sub> decreases with increasing alkali concentration. During the geopolymerization process, the sulfate ions from SO<sub>3</sub> present in the granulated blast furnace slag (GBFS) react with the pollutants, forming sulfate-bearing phases that stabilize the contaminants. Consequently, the SO<sub>3</sub> content is reduced with higher NaOH concentrations [38]. Other oxides appear to have little to no influence on the geopolymerization process.

### 3.4 Fourier Transform Infrared Spectroscopy (FTIR)

The variations in chemical groups during the solidification of landfill leachate by the geopolymer were investigated using FTIR, as indicated by Fig. 4. The FTIR spectra of geopolymers differed significantly from those of raw GBFS, denoting the creation of a new stage throughout geopolymerization. The primary geopolymer peaks at around  $1000\text{ cm}^{-1}$  portray the Si-O-Al absorption bands (Medina et al., [47]). This is seen in 3 M and 12 M geopolymers; the broadness in 3 M was large, with a wavenumber of  $948.24\text{ cm}^{-1}$ , whereas the broadness in 6 M is  $933\text{ cm}^{-1}$ , indicating that the aluminium is substituted for Silicon, indicating that landfill leachate increases the extent of geopolymerization [19]. The symmetric stretching of Si-Al-O is represented by the bands  $750\text{--}765\text{ cm}^{-1}$  [18]. The vibrations in the weak bonds of silanol (Si-OH) and aluminol (Al-OH) in 3 M and 12 M induce the bands at  $1675\text{--}1686\text{ cm}^{-1}$  [30]. The broadness disappears as the concentration increases. The O-C-O vibration of  $\text{CO}_3^{2-}$  induced the peak at  $1405\text{ cm}^{-1}$ , illustrating the presence of inorganic carbon in the samples [2]. There are no similar trends in the FT-IR for increasing concentration, indicating that the inclusion of landfill leachate concentration significantly impacts the geopolymer structure.

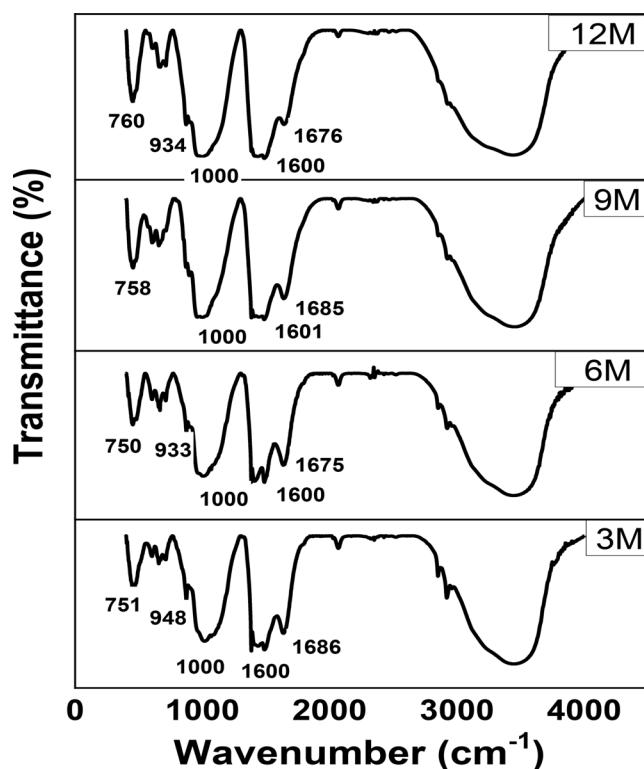


Fig. 4 FTIR spectra for varying activator concentrations

### 3.5 X-Ray Diffraction (XRD)

Figure 5 shows the XRD for raw GBFS and GBFS-based geopolymers at varying concentrations. It is visible that the XRD patterns are all amorphous. The XRD results of raw GBFS show a broad diffuse hump around  $23^{\circ}\text{--}36^{\circ}$ , indicating that it is primarily clear and bright amorphous with magnetite and a huge portion of silica as a type of quartz. This finding is consistent with past research by (Huseien et al., 2016). The clear and bright nature of the GBFS facilitates alkali activation; as the concentration increases, the alkaline activator creates a CSH that coincides with the amorphous gel. CSH and CASH gels are used in the alkali activation of GBFS. The XRD results upon alkaline activation revealed a broad and amorphous hump at  $20^{\circ}\text{--}40^{\circ}$ , confirming the formation of CSH and CAH. The CSH and CAH stages are in charge of creating a zeolite, primarily composed of alumina-silicates with  $\text{SiO}_4$  and  $\text{AlO}_4$  structures linked by common  $\text{O}_2$  atoms. The findings are consistent with those published by [12, 49], who discovered that forming CSH phases contributes to the strength and durability formed in geopolymer. The creation of geopolymer products was also indicated by the emergence of new peaks on the amorphous hump at  $28^{\circ}\text{--}30^{\circ}$  designated to the badly crystalline structure of CSH, calcite, and CAH (Phummiphan et al., [48]). CSH is responsible for the formation of peaks at  $5^{\circ}$  after geopolymerisation (3 M, 6 M, 9 M, and 15 M). It has been reported that CSH with a low C/S ratio is the most common moisture product of GBFS geopolymerisation (Ahmari and Zhang, [50]). Crystalline are very equivalent in all 4 geopolymer specimens (3 M, 6 M, 9 M, and 12 M). Adjustments in the chemical composition of the gels witnessed over time happen in the amorphous state of the specimens, with few crystalline developments in specimens with greater alkaline concentrations. This is due to the amorphous state of the geopolymer gels, which makes characterization with XRD analysis difficult.

### 3.6 Scanning Electron Microscopic (SEM)

SEM micrographs of raw GBFS and GBFS-based geopolymers made at various alkali concentrations (3 M, 6 M, 9 M, and 12 M) are shown in Fig. 6. GBFS has a diverse morphology and is very permeable to water. The micrographs of GBFS-based geopolymers produced at various alkali concentrations show not to be permeable to water due to the inclusion of NaOH, in which the structure resulted to be very close-packed and plain with good space-filling characteristics because of the development of CSH and CAH gel; these findings are in line with the XRD results. The largest UCS obtained is explained by the plain/close-packed matrix at 12 M. Zeolites appear as greyish white and major

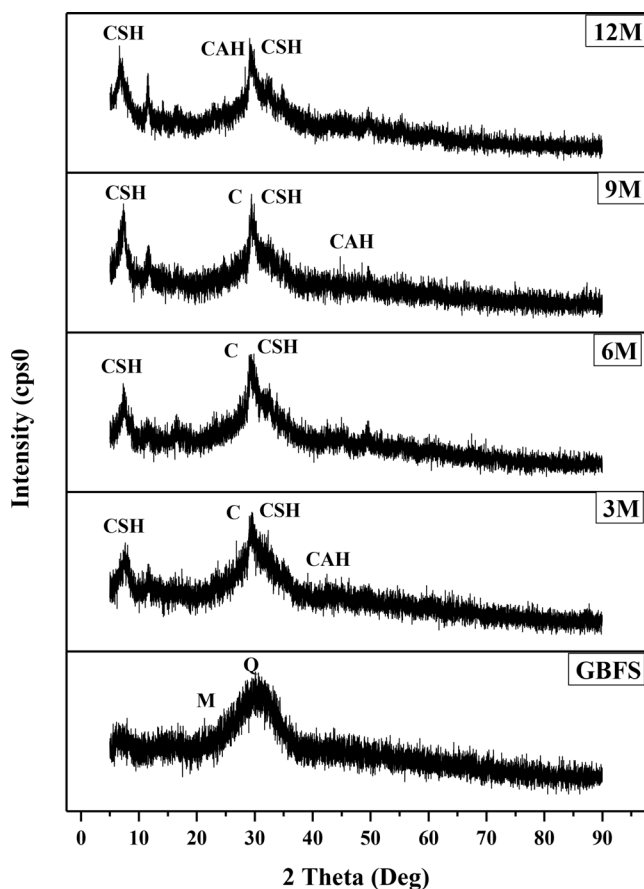


**Fig. 5** XRD pattern of raw GBFS and GBFS-based geopolymer at different alkali concentrations (M=Magnetite, Q=Quartz, CSH=Calcium silicate hydrate, CAH=Calcium aluminate hydrate, C=Calcite)

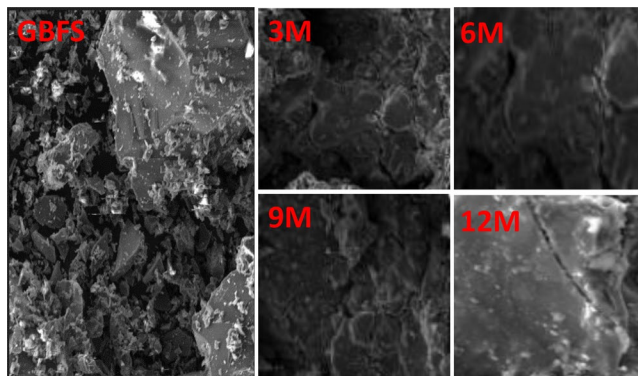


**Fig. 6** SEM micrographs of GBFS-geopolymers at different activator concentrations

constituent on the exterior of all GBFS geopolymer specimens, resulting in increased UCS. Because of the lower concentration, a few undissolved particulates on the specimens precipitated rather than condensing into CSH and CAH gel, arising in a weakened geopolymer paste. The GBFS granules lead to cracks as more Silicon and Aluminum are dissolved in the alkaline environment, thereby expanding the

**Table 2** Leaching test results of geopolymer at 3 and 7 curing days

Pollutants	3 days geopolymer (mg/L)	7 days geopolymer (mg/L)	Allowable concentration in leachate (mg/L) by the USEPA
Cd	0.003	0.005	1
Pb	0.004	0.006	5
Cr	0.005	0.002	5
As	0.031	0.010	5

surface area for geopolymerisation. Higher concentrations of 12 M have the highest density structure, indicating good geopolymerisation and, thus the highest UCS.

### 3.7 TCLP

Table 2 shows the TCLP assessment for geopolymers made with leachate for 3- and 7-day specimens. According to the TCLP outcomes, the GBFS metal concentration did not surpass the USEPA metal concentration limit. The TCLP findings align with previous research [40]. This indicates that the GBFS geopolymer was successful in stabilizing the pollutants present in the landfill leachate.

## 4 Conclusion

This research aimed to use alkali-activated blast furnace slag-based geopolymers to solidify landfill leachates. The study was conducted to determine the influence of alkali content, L/S ratio and curing time on compressive strength, the impact of L/S ratio on flow workability, UCS characteristics of blast furnace slag geopolymer using microstructural examination, XRF, FTIR, XRD, SEM were analysed, and a TCLP was done. The findings generate the following conclusions. Because of higher levels of silica and alumina leaching, increasing the NaOH solution concentration leads to a rise in UCS of the alkali-activated GBFS-based samples out of 3 M, 6 M, 9 M, and 12 M, 12 M had a highest UCS of 45.738 MPa. After solidifying/stabilizing LLC, the L/S ratio substantially influences the UCS of GBFS-based geopolymers. With a UCS of 45.738 MPa at 12 M, the 15% L/S ratio had the best workability. According to the results, the best curing time is 7 days because the development of UCS and the curing time have a direct proportionality relationship. The L/S ratio and flow workability have a linear relationship. The maximum flow workability had an average diameter of 242 mm for 0.25, but a minimum L/S of 0.15 was required to obtain a workable GBFS mortar. The XRF results showed that GBFS revealed hydraulic cementitious features. There was no similar trend in the FT-IR for the increasing concentration, denoting that the inclusion of landfill leachate concentration significantly affects the

structure of the geopolymer. Because the GBFS metal concentration did not surpass the USEPA metal concentration limit, the TCLP demonstrated that the created geopolymer brick is eco-sustainable and could be categorized as a green construction brick.

**Acknowledgements** The author would like to thank the University of Johannesburg URC grant number 2023URC00710 the National Research Foundation of South Africa Grant Unique Number TTK2205067264 for providing the resources to conduct the study.

**Funding** Open access funding provided by University of Johannesburg.

**Data availability** All relevant data is included within the article.

## Declarations

**Competing Interest** There were no competing interests or other relationships that influenced the authors on this paper.

**Open Access** This article is licensed under a Creative Commons Attribution 4.0 International License, which permits use, sharing, adaptation, distribution and reproduction in any medium or format, as long as you give appropriate credit to the original author(s) and the source, provide a link to the Creative Commons licence, and indicate if changes were made. The images or other third party material in this article are included in the article's Creative Commons licence, unless indicated otherwise in a credit line to the material. If material is not included in the article's Creative Commons licence and your intended use is not permitted by statutory regulation or exceeds the permitted use, you will need to obtain permission directly from the copyright holder. To view a copy of this licence, visit <http://creativecommons.org/licenses/by/4.0/>.

## References

- Aderemi AO, Oriaku AV, Adewumi GA, Otitolaju AA (2011) Assessment of groundwater contamination by leachate near a municipal solid waste landfill. *Afr J Environ Sci Technol* 5(11):933–940
- Aziz IH, Abdullah MMAB, Mohd Salleh MAA, Azimi EA, Chaiprapa J, Sandu AV (2020) Strength development of solely ground granulated blast furnace slag geopolymers. *Constr Build Mater* 250:p118720. <https://doi.org/10.1016/j.conbuildmat.2020.118720>
- Azzahrán Abdullah SF, Yun-Ming L, Al Bakri MM, Cheng-Yong H, Zulkifly K, Hussin K (2018) Effect of Alkali Concentration on Fly Ash Geopolymers. *IOP Conference Series: Materials Science and Engineering*, 343, p.012013. <https://doi.org/10.1088/1757-899x/343/1/012013>
- Baloyi O et al (2012) National waste information baseline report. Department of Environmental Affairs, Pretoria
- Butt TE, Clark M, Coulon F, Oduyemi KO (2009) A review of literature and computer models on exposure assessment. *Environ Technol* 30(14):1487–1501
- Chindaprasirt P, Buapa N, Cao HT (2005) Mixed cement containing fly ash for masonry and plastering work. *Constr Build Mater* 19(8):612–618. <https://doi.org/10.1016/j.conbuildmat.2005.01.009>
- Conner JR (1990) Chemical fixation and solidification of hazardous wastes. Van Nostrand Reinhold New York, s.l.
- Das SK, Mustakim SM, Adesina A, Mishra J, Alomayri TS, Assaedi HS, Kaze CR (2020) Fresh, strength and microstructure properties of geopolymer concrete incorporating lime and silica fume as replacement of fly ash. *J Building Eng* 32:101780. <https://doi.org/10.1016/j.jobbe.2020.101780>
- Deng W et al (2022) Solidification/Stabilization of MSWI fly Ash using a Novel Metallurgical Slag-based Cementitious Material. *Minerals* 12(5):599
- Dharmarathne N, Gunatilake J (2013) Leachate characterization and surface groundwater pollution at municipal solid waste landfill of Gohagoda, Sri Lanka. *Int J Sci Res* 3(11):1–7
- El-Gohary FA, Kamel G (2016) Characterization and biological treatment of pre-treated landfill leachate. *Ecol Eng* Volume 94:268–274
- Falayi T (2019) Sustainable solidification of ferrochrome slag through geopolymerisation: a look at the effect of curing time, type of activator and liquid solid ratio. *Sustainable Environ Res* 29(1). <https://doi.org/10.1186/s42834-019-0022-7>
- Falayi T, Okonta FN, Ntuli F (2017) Desilication of fly ash and development of lightweight construction blocks from alkaline activated desilicated fly ash. *Int J Environ Waste Manag* 20(3):233. <https://doi.org/10.1504/ijewm.2017.087152>
- Güllü H, Agha AA (2021) The rheological, fresh and strength effects of cold-bonded geopolymer made with metakaolin and slag for grouting. *Constr Build Mater* 274:122091
- Hunce SY, Akgul D, Demir G, Mertoglu B (2012) Solidification/stabilization of landfill leachate concentrate using different aggregate materials. *Waste Manag* 32(7):1394–1400
- Jafari Nadoushan M, Ramezaniyanpour AA (2016) The effect of type and concentration of activators on flowability and compressive strength of natural pozzolan and slag-based geopolymers. *Constr Build Mater* 111:337–347. <https://doi.org/10.1016/j.conbuildmat.2016.02.086>
- Jin F, Wang F, Al-Tabbaa A (2016) Three-year performance of in-situ solidified/stabilised soil using novel MgO-bearing binders. *Chemosphere* 144:681–688
- Karthik A, Sudalaimani K, Vijayakumar CT, Saravanakumar SS (2019) Effect of bio-additives on physicochemical properties of fly ash-ground granulated blast furnace slag based self-cured geopolymer mortars. *J Hazard Mater* 361:56–63. <https://doi.org/10.1016/j.jhazmat.2018.08.078>
- Li J, Sun P, Li J, Lv Y, Ye H, Shao L, Du D (2020) Synthesis of electrolytic manganese residue-fly ash-based geopolymers with high compressive strength. *Constr Build Mater* 248:118489. <https://doi.org/10.1016/j.conbuildmat.2020.118489>
- Huseien Q, Cui H, Li Y, Song X, Liu W, Wang Y, Hou H, Zhang H, Li Y, Wang F, Song J (2023) Challenges and engineering application of landfill leachate concentrate treatment—*Environmental Research*, p.116028
- Liew YM, Kamarudin H, Bakri AMMA, Binhussain M, Luqman M, Nizar IK, Ruzaidi CM, Heah CY (2011) Influence of solids-to-liquid and activator ratios on Calcined Kaolin Cement Powder. *Physics Procedia* 22:312–317. <https://doi.org/10.1016/j.phpro.2011.11.049>
- Liu Q, Wang X, Gao M, Guan Y, Wu C, Wang Q, Rao Y, Liu S (2022) Heavy metal leaching behaviour and long-term environmental risk assessment of cement-solidified municipal solid waste incineration fly ash in a sanitary landfill. *Chemosphere* 300:p134571
- Magaji J (2012) Effects of waste dump on the quality of plants cultivated around Mpape dumpsite FCT Abuja, Nigeria. *Ethiop J Environ Stud Manage* 5(4):567–573
- Mahmoodi O, Siad H, Lachemi M, Dadsetan S, Sahmaran M (2020) Development of ceramic tile waste geopolymer



- binders based on pre-targeted chemical ratios and ambient curing. *Constr Build Mater* 258:120297. <https://doi.org/10.1016/j.conbuildmat.2020.120297>
25. Mohd Mortar NA, Abdullah MMAB, Abdul Razak R, Rahim A, Aziz SZ, Nabialek IH, Jaya M, Semenescu RP, Mohamed A, R. and, Ghazali MF (2022) Geopolymer ceramic application: A review on mix design, properties and reinforcement enhancement. *Materials*, 15(21), p.7567
  26. Nahman A (2011) Pricing landfill externalities: emissions and disamenity costs in Cape Town, South Africa. *Waste Manag* 31(9–10):2046–2056
  27. Omran A, Gavrilescu M (2008) Municipal solid waste management in developing countries: A Perspective on vietnam. *Environ Eng Manage J (EEMJ)*, 7(4)
  28. Part WK, Ramli M, Cheah CB (2015) An overview on the influence of various factors on the properties of geopolymer concrete derived from industrial by-products. *Constr Build Mater* 77:370–395. <https://doi.org/10.1016/j.conbuildmat.2014.12.065>
  29. Pollard S, Montgomery D, Sollars C, Perry R (1991) Organic compounds in the cement-based stabilisation/solidification of hazardous mixed wastes—mechanistic and process considerations. *J Hazard Mater* 28:313–327
  30. Prusty JK, Pradhan B (2020) Multi-response optimization using Taguchi-Grey relational analysis for composition of fly ash-ground granulated blast furnace slag based Geopolymer concrete. *Constr Build Mater* 241:118049. <https://doi.org/10.1016/j.conbuildmat.2020.118049>
  31. Samantasinghar S, Singh SP (2018) Effect of synthesis parameters on compressive strength of fly ash-slag blended geopolymer. *Constr Build Mater* 170:225–234. <https://doi.org/10.1016/j.conbuildmat.2018.03.026>
  32. Sholichin M (2012) Field investigation of groundwater contamination from solid waste landfill in Malang, Indonesia. *Int J Civil Environ Eng* 12:74–83
  33. Sithole N, Okonta F, Ntuli F (2019) Development of lightweight construction blocks by alkaline activation of bof slag. *J Solid Waste Technol Manage* 45(2):175–185
  34. Sithole NT, Mashifana T (2020) Geosynthesis of building and construction materials through alkaline activation of granulated blast furnace slag. *Constr Build Mater* 264:p120712. <https://doi.org/10.1016/j.conbuildmat.2020.120712>
  35. Sithole NT, Okonta F, Ntuli F (2020) Mechanical properties and structure of fly Ash Modified Basic Oxygen furnace slag based Geopolymer Masonry blocks. *J Solid Waste Technol Manage* 46(3):372–383. <https://doi.org/10.5276/jswtm/2020.372>
  36. Talalaj IA (2015) Mineral and organic compounds in leachate from landfill with concentrate recirculation. *Environ Sci Pollut Res* 22(4):2622–2633
  37. Thakur IS, Das MT, Ghosh P (2014) InÂ vitro toxicity evaluation of organic extract of landfill soil and its detoxification by indigenous pyrene-degrading *Bacillus* sp. ISTPY1. *International Biodeterioration & Biodegradation*
  38. Usta MC, Yörük CR, Uibu M, Traksmaa R, Hain T, Gregor A, Trikkel A (2023) Carbonation and leaching behaviors of cement-free monoliths based on high-sulfur fly ashes with the incorporation of Amorphous Calcium Aluminate. *ACS Omega* 8(32):29543–29557
  39. Wardhono A, Law DW, Strano A (2015) The strength of Alkali-activated Slag/fly Ash Mortar Blends at ambient temperature. *Procedia Eng* 125:650–656. <https://doi.org/10.1016/j.proeng.2015.11.095>
  40. Yahya Z, Abdullah M, Hussin K, Ismail K, Razak R, Sandu A (2015) Effect of Solids-To-Liquids, Na<sub>2</sub>SiO<sub>3</sub>-To-NaOH and curing temperature on the Palm Oil Boiler Ash (Si+ca) Geopolymerisation System. *Materials* 8(5):2227–2242. <https://doi.org/10.3390/ma8052227>
  41. Ye J, Zhang W, Shi D (2014) Effect of elevated temperature on the properties of geopolymer synthesized from calcined ore-dressing tailing of bauxite and ground-granulated blast furnace slag. *Constr Build Mater* 69:41–48. <https://doi.org/10.1016/j.conbuildmat.2014.07.002>
  42. Zhang S, Zhao Y, Guo Z, Ding H (2021) Stabilization/solidification of hexavalent chromium-containing tailings using low-carbon binders for cemented paste backfill. *J Environ Chem Eng* 9(1):104738
  43. Zhang H, Ji Z, Zeng Y, Pei Y (2022) Solidification/stabilization of landfill leachate concentrate contaminants using solid alkali-activated geopolymers with a high liquid solid ratio and fixing rate. *Chemosphere* 288(Pt 2):132495
  44. Zhang H, Gao S, Ji Z, Cui J, Pei Y (2023) Solidification/stabilization of organic matter and ammonium in high-salinity landfill leachate concentrate using one-part fly ash-based geopolymers. *J Environ Chem Eng* 11(2):109379.
  45. USEPA (1992) Method 1311, Toxicity Characteristic Leaching Procedure (TCLP). Publication SW–846: test methods for evaluating solid waste, physical/chemical methods. [www.epa.gov/epaoswer/hazwaste/test/pdfs/1311.pdf](http://www.epa.gov/epaoswer/hazwaste/test/pdfs/1311.pdf)
  46. Yildirim G, Aras GH, Banyhussan QS, Şahmaran M, Lachemi M (2015) Estimating the self-healing capability of cementitious composites through non-destructive electrical-based monitoring. *Ndt & E Int* 76:26–37.
  47. Madani H, Ramezani-pour AA, Shahbazinia M, Ahmadi E (2020) Geopolymer bricks made from less active waste materials. *Constr Build Mater* 247:118441.
  48. Phummiphan I, Horpibulsuk S, Rachan R, Arulrajah A, Shen SL, Chindapasirt P (2018) High calcium fly ash geopolymer stabilized lateritic soil and granulated blast furnace slag blends as a pavement base material. *J Hazard Mater* 341:257–267.
  49. Suwan T, Fan M (2014) Influence of OPC replacement and manufacturing procedures on the properties of self-cured geopolymer. *Constr Build Mater* 73:551–561.
  50. Ahmari S, Zhang L (2013) Durability and leaching behavior of mine tailings-based geopolymer bricks. *Constr Build Mater* 44:743–750.

**Publisher's Note** Springer Nature remains neutral with regard to jurisdictional claims in published maps and institutional affiliations.